the choice of an adjoint field which satisfies part of the required boundary conditions. In the numerical analysis, the resulting matrix is considerably reduced (for example, compared with [3]). The computation time is also largely reduced by taking the Maclaurin series expansion forms of the infinite sums.

The formulation shown here is rather general. It can in principle be applied to various structures involving inhomogeneous dielectric media (e.g., multiconductor transmission lines in multilayered dielectric media). Finite metallization thickness can also be considered with a modified choice of the contour as already suggested in [3].

REFERENCES

[1] T. Honma and I. Fukai, "An analysis for the equivalence of boxed and shielded strip lines by a boundary element method," *Trans. IECE Japan*, vol. J65-B, pp. 497–498, 1982.

[2] M. Ikeuchi, "Boundary element analysis of shielded microstrip lines with dielectric layers," *Trans. IECE Japan*, vol. J67-E, no. 11, pp. 585–590, 1984.

[3] T. N. Chang and C. H. Tan, "Analysis of a shielded microstrip line with finite metallization thickness by the boundary element method," *IEEE Trans. Microwave Theory Tech.*, vol. 38, no. 8, pp. 1130–1132, 1990.

[4] V. Postoyalko, "Green's function treatment of edge singularities in the quasi-TEM analysis of microstrip," *IEEE Trans. Microwave Theory Tech.*, vol. 34, no. 11, pp. 1092–1095, 1986.

[5] B. Bhat and S. K. Koul, "Unified approach to solve a class of strip and microstrip-like transmission lines," *IEEE Trans. Microwave Theory Tech.*, vol. 30, no. 5, pp. 679–685, 1982.

[6] R. E. Collin, *Field Theory of Guided Waves* New York: McGraw-Hill, 1960, pp. 52–54, pp. 576–581.

[7] T. Itoh, "A method for analyzing shielded microstrip lines," *Trans IECE, Japan*, vol. j58-B, pp. 24–29, Jan. 1975.

CAD of T-Septum Waveguide Evanescent-Mode Filters

Vladimir A. Labay and Jens Bornemann

Abstract— This paper presents a mode-matching-based design of evanescent-mode waveguide filters with T-septum shaped metal inserts. Owing to the wideband characteristics of the T-septum waveguide, the proposed design constitutes a significant improvement over common evanescent-mode filters with respect to both size reduction and stopband behavior. The theoretical approach is verified at the example of a three-resonator 8.8-GHz filter prototype of less than 3/4 inch length. The second passband is beyond 27 GHz. Since the design procedure takes higher-order mode interactions into account, good agreement between theory and experiment is obtained over the entire measurement range between 8.2 and 40 GHz.

I. INTRODUCTION

Evanescent-mode filters are constructed from resonators within a below-cutoff waveguide section and rectangular waveguide discontinuities for connection to a standard-size input/output guide [1]–[5]. The resonators are formed by introducing appropriate obstacles such as capacitive screws [1], round posts [2], dielectric blocks [3], ridges

[4] or E-plane fins [5] at suitable intervals along the below-cutoff section. While in a given frequency band, the filter response improves with reducing the size of the evanescent-mode guide, two problems are immediately associated with the resonators of such filters. First, their cross-sections need to be specifically shaped in order to allow for a considerable reduction in cutoff frequency and, secondly, simplicity in shape must be maintained to apply efficient computer-aided modelling and design procedures. A structure, which satisfies these requirements but has not yet been used in evanescent-mode configurations, is the T-septum waveguide, e.g., [6].

Therefore, this paper focuses on the computer-aided design of T-septum waveguide evanescent mode filters. By incorporating the T-septum eigenfunctions [7] into a mode-matching-based design routine [8], higher-order mode interactions at all discontinuities are included, thus resulting in close agreement between predicted and measured filter responses. Another advantage of this design is its remarkably small size.

II. THEORY

The mode-matching technique is applied to calculate the generalized scattering matrix of the T-septum waveguide evanescent-mode filter. The electromagnetic field in each longitudinal filter section is derived from the z-components of the magnetic and electric vector potential. Since the method of analysis together with the potential and eigenfunctions of the rectangular waveguide sections are already given in [8], only the T-septum waveguide cross-section functions need to be presented here. Choosing the subregion division of the cross-section according to Fig. 1 and applying electric and magnetic wall symmetry at $y = 0$ and $x = a/2$, respectively, the cross-section functions yield:

$$T_h(x,y) = \sum_{l=0}^{L-1} A_l^I \frac{\sin\left\{k_{xl}^I\left(x - \frac{a}{2}\right)\right\}}{k_{xl}^I} \frac{\cos\left\{\frac{l\pi}{b_1}y\right\}}{\sqrt{1 + \delta_{0l}}}$$
$$+ \sum_{m=0}^{M-1} A_m^{II} \cos\{k_{xm}^{II}x\} \frac{\cos\left\{\frac{2m\pi}{b}y\right\}}{\sqrt{1 + \delta_{0m}}}$$
$$+ \sum_{n=0}^{N-1} A_n^{III} \cos\{k_{xn}^{III}(x - a_2)\} \frac{\cos\left\{\frac{n\pi}{b-b_2}(y-b_2)\right\}}{\sqrt{1 + \delta_{0n}}}$$
(1)

$$T_e(x,y) = \sum_{l=1}^{L-1} D_l^I \cos\left\{k_{xl}^I\left(x - \frac{a}{2}\right)\right\} \sin\left\{\frac{l\pi}{b_1}y\right\}$$
$$+ \sum_{m=1}^{M-1} D_m^{II} \frac{\sin\{k_{xm}^{II}x\}}{k_{xm}^{II}} \sin\left\{\frac{2m\pi}{b}y\right\}$$
$$+ \sum_{n=1}^{N-1} D_n^{III} \frac{\sin\{k_{xn}^{III}(x - a_2)\}}{k_{xn}^{III}} \sin\left\{\frac{n\pi}{b-b_2}(y-b_2)\right\}$$
(2)

Amplitude coefficients A^i, D^i and separation constants $k_x^i (i \in [I, II, III])$ are determined by the solution of the characteristic matrix equation [7] and subsequent power normalization [8]. The generalized scattering matrix of the overall structure is obtained by cascading the individual scattering matrices of the discontinuities and homogeneous sections involved, e.g., [8]. Sufficient convergence behavior is obtained with 35 TE and TM modes, $M = 20$ expansion
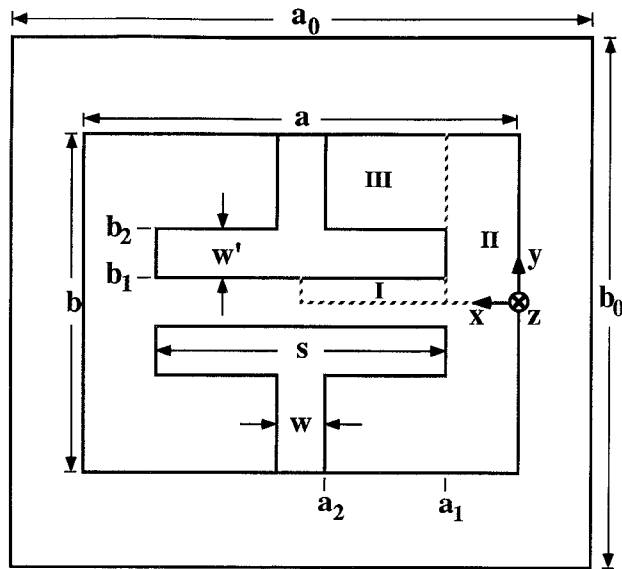
Fig. 1. Cross-section dimensions of T-septum waveguide filter.

terms, and L and N chosen according to the y-direction dimensions ratios (c.f. Fig. 1) of the subregions [9]. The CPU time for the analysis of one set of filter parameters is about 10 minutes on an IBM RISC station.

The design of the T-septum waveguide evanescent-mode filter is carried out in four steps. First, the below-cutoff guide dimensions are selected for a fundamental-mode cutoff at approximately twice the midband frequency of the filter. Second, the dimensions of the T-septum are determined to provide a cutoff frequency at approximately that of the input/output guide. Third, assuming as a rough approximation that the behavior for the below-cutoff coupling sections is purely inductive, the number of resonators as well as the initial lengths of T-septum and below-cutoff sections can be calculated using standard filter theory and impedance inverters [10]. Fourth, the individual section lengths are systematically altered by optimization procedures, e.g., [11], to approximate the specified filter characteristic. Note that in steps two to four, the numerical analysis technique must be applied iteratively to meet given specifications.

III. RESULTS

The calculated response of a Q-band millimeter-wave filter at 41 GHz is shown in Fig. 2. Although the cutoff frequency of the reduced-size waveguide is 73.8 GHz, the second passband is shifted beyond 92 GHz. The dashed lines demonstrate the important feature that the filter maintains its excellent stopband characteristics even if a propagating higher-order mode of identical field symmetry is excited in the input/output guide (beyond 79 GHz).

In order to verify the computer-aided analysis and design procedure, the theoretically predicted filter is compared with measured results of a three-resonator X-band prototype (Fig. 3). The differences in the passband response (inset of Fig. 3) are caused by severe limitations in the manufacturing process. Surface roughness and an off-center connection between the X-band waveguide and the below-cutoff structure contribute to insertion and return loss values of 1.8 dB and 13 dB, respectively. The axial misalignment is clearly indicated by the measured insertion loss peak at 13 GHz, the TE_{20}-mode cutoff frequency of the feeding X-band waveguide. Since such offsets have purposely been omitted in the theory in order to simplify the design procedure and to reduce the CPU time, the peak at 13 GHz is not reproduced in the theoretical curve. Beyond 12.4 GHz, a series of
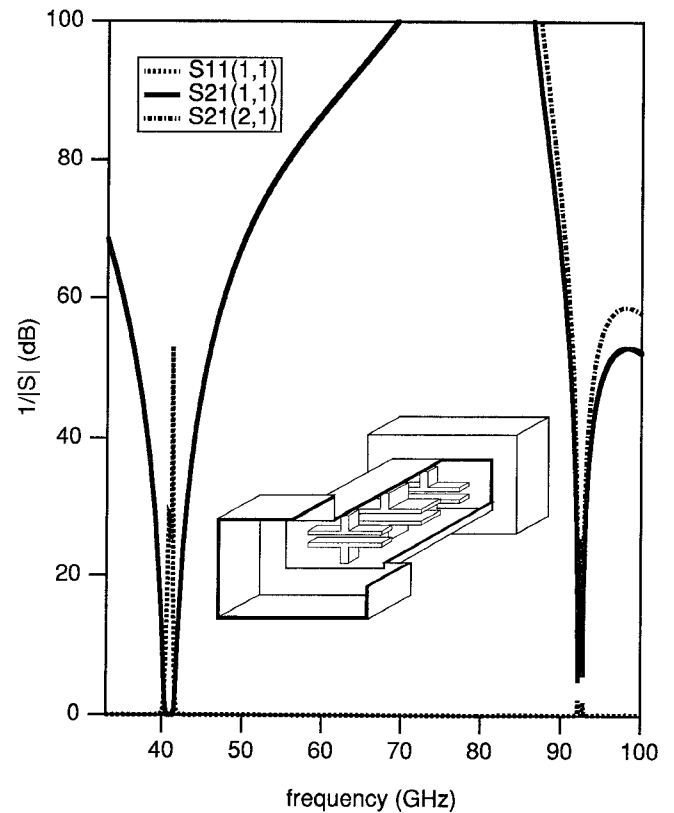
Fig. 2. Calculated response of a three-resonator evanescent-mode T-septum waveguide filter for Q-band application. Cross-section dimensions (c.f. Fig. 1): $a_0 = 5.69$ mm, $b_0 = 2.845$ mm, $a = 2.032$ mm, $b = 1.016$ mm, $s = 1.632$ mm, $w = 0.4$ mm, $w' = 0.2$ mm, $b_1 = 0.08$ mm; section lengths (c.f. Fig. 4, l_R = T-septum waveguide length, $l_{C'}$ = below-cutoff waveguide length): $l_{C1} = l_{C4} = 0.16$ mm, $l_{R1} = l_{R3} = 0.128$ mm, $l_{C2} = l_{C3} = 2.55$ mm, $l_{R2} = 0.238$ mm.
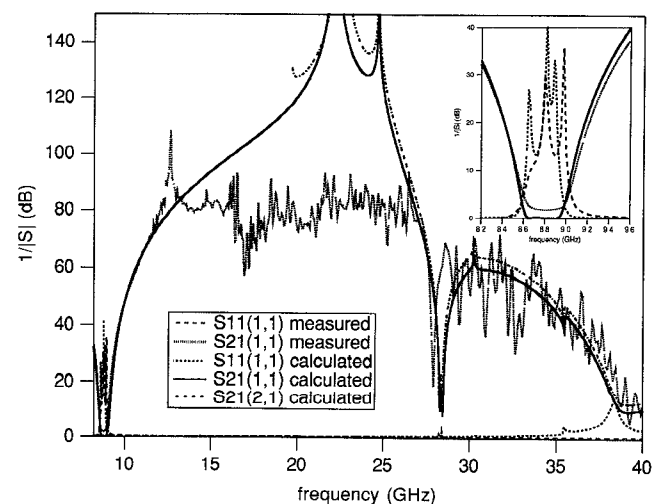
Fig. 3. Comparison between measured and calculated response of an X-band three-resonator filter prototype. Cross-section dimensions (c.f. Fig. 1): $a_0 = 22.86$ mm, $b_0 = 10.16$ mm, $a = 7\,0$ mm, $b = 6.95$ mm, $s = 5.12$ mm, $w = 2.02$ mm, $w' = 1.02$ mm, $b_1 = 0.3$ mm; section lengths (c.f. Fig. 4, l_R = T-septum waveguide length, l_C = below-cutoff waveguide length): $l_{C1} = l_{C4} = 0.54$ mm, $l_{R1} = l_{R3} = 0.50$ mm, $l_{C2} = l_{C3} = 7.68$ mm, $l_{R2} = 0.90$ mm.

waveguide transformers have been used to extend the measurements to 40 GHz. Overmoding in the X-band input/output guides seems to
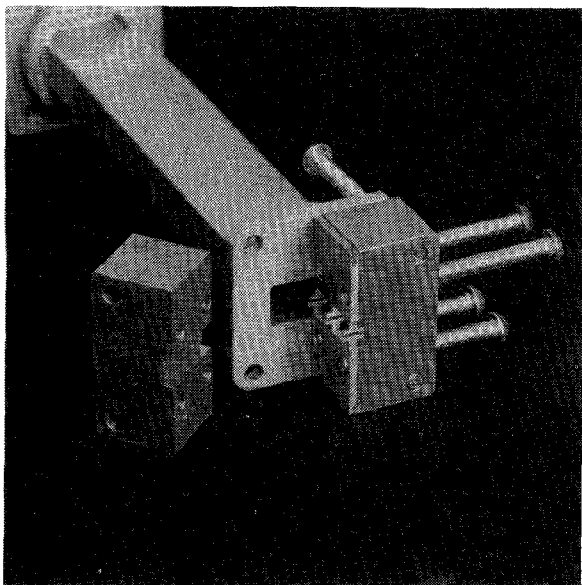
Fig. 4. Photograph of the opened evanescent-mode T-septum waveguide filter prototype with feeding X-band waveguide.

be responsible for the measured noise at beyond-X-band frequencies. Except for these limitations, however, close agreement between theoretical and experimental data is obtained over the entire measured frequency range. This indicates that a fabrication procedure utilizing modern production facilities will cause the evanescent-mode filter to respond as predicted.

Fig. 4 shows a photograph of the opened evanescent-mode T-septum waveguide filter prototype with the feeding X-band waveguide. A split-block waveguide housing is used to sandwich the two T-septum inserts. Note that due to the high bandwidth of the T-septum waveguide, i.e., its capability to significantly reduce the cutoff frequency compared to a ridge waveguide of identical housing dimensions, the filter component is extremely small. With an overall length of less than 3/4 inches, this design is one of the most space-efficient bandpass configurations proposed so far in waveguide technology.

IV. CONCLUSIONS

The theoretical treatment of the T-septum waveguide by mode-matching techniques forms a powerful tool for the computer-aided design of evanescent-mode filter applications. Through the incorporation of higher-order mode interactions, the proposed model provides design data which are in close agreement with experiments as is demonstrated at the example of an X-band filter prototype. The broadband characteristics of the T-septum waveguide make it possible, first, to improve the stopband behavior compared to common evanescent-mode configurations and, secondly, to reduce the filter size considerably. The length of the three-resonator prototype measures approximately one third of the guide wavelength at midband frequency.

REFERENCES

[1] G. Craven and C. K. Mok, "The design of evanescent mode waveguide band-pass filters for a prescribed insertion loss characteristic," *IEEE Trans. Microwave Theory Tech.*, vol. MTT-19, pp. 295–308, Mar. 1971.

[2] H. F. Chappell, "Waveguide low pass filter using evanescent mode inductors," *Microwave J.*, vol. 21, pp. 71–72, Dec. 1978.
[3] R. Vahldieck and W. J. R. Hoefer, "Computer-aided design of dielectric resonator filters in waveguide sections below cutoff," *Electron. Lett.*, vol. 21, pp. 843–844, Sept. 1985.
[4] J.-W. Tao and H. Baudrand, "Multimodal variational analysis of uniaxial waveguide discontinuities," *IEEE Trans. Microwave Theory Tech.*, vol. 39, pp. 506–516, Mar. 1991.
[5] Q. Zhang and T. Itoh, "Computer-aided design of evanescent-mode waveguide filters with non-touching E-plane fins," *IEEE Trans. Microwave Theory Tech.*, vol. 36, pp. 404–412, Feb. 1988.
[6] Y. Zhang and W. T. Joines, "Some properties of T-septum waveguides," *IEEE Trans. Microwave Theory Tech.*, vol. MTT-35, pp. 769–775, Aug. 1987.
[7] V. A. Labay and J. Bornemann, "Singular value decomposition improves accuracy and reliability of T-septum waveguide field-matching analysis," *Int. J. MIMICAE*, vol. 2, pp. 82–89, Apr. 1992.
[8] J. Bornemann and F. Arndt, "Transverse resonance, standing wave, and resonator formulations of the ridge waveguide eigenvalue problem and its application to E-plane finned waveguide filters," *IEEE Trans. Microwave Theory Tech.*, vol. 38, pp. 1104–1113, Aug. 1990.
[9] Y. C. Shih, "The mode-matching method," in *Numerical Techniques For Microwave And Millimeter-Wave Passive Structures*, T. Itoh, Ed., New York: Wiley, 1989, ch. 9.
[10] L. Q. Bui, D. Ball and T. Itoh, "Broad-band millimeter-wave E-plane bandpass filters," *IEEE Trans. Microwave Theory Tech.*, vol. MTT-32, pp. 1655–1658, Dec. 1984.
[11] J. W. Bandler and S. H. Chen, "Circuit optimization: The state of the art," *IEEE Trans. Microwave Theory Tech.*, vol. 36, pp. 424–443, Feb. 1988.

Asymptotic Analysis of Mode Transition in General Class of Circular Hollow Waveguides at the Infrared Frequency

Yuji Kato and Mitsunobu Miyagi

Abstract—Correspondence between hybrid modes in small and large core circular hollow waveguides is discussed by using an asymptotic theory for the infrared. The mode changes or mode transitions in several hollow waveguides are discussed which depend on the cladding material and the mode order. For the dielectric-coated metallic waveguides, mode changes also depend on the thickness of the coated dielectric. For the singly cladded hollow waveguides, the region is shown in the plane of complex refractive index $(n - jk)$ of cladding material where the HE_{11} mode in large core waveguides approaches the TE or TM mode.

I. INTRODUCTION

Hollow waveguides are important media in the wavelengths where bulky losses of materials are too high to achieve low-loss flexible fibers and also media for high-powered laser light transmission where the reflections at input and output ends of waveguides can be neglected [1]. Therefore, the waveguides have been recently regarded a candidate for high-powered CO_2 laser light [2] and infrared radiometry [3].

Mode properties of circular hollow waveguides were already discussed in detail [1] when the core diameter is large. Due to needs